Biomarkers and Heterogeneous Fibroblast Phenotype Associated with Incisional Hernia

Devendra K. Agrawal (DAgrawal@WesternU.edu)
Western University of Health Sciences https://orcid.org/0000-0001-5445-0013
Finosh G. Thankam
Western University of Health Sciences
Nicholas K. Larsen
Creighton University School of Medicine
Ann Verghese
Creighton University School of Medicine
Thao-Nguyen Bui
Creighton University School of Medicine
Robert J Fitzgibbons
Creighton University School of Medicine

Research Article

Keywords: Incisional Hernia, Fibroblasts, Biomarkers, ECM pathology, Laparotomy, Wound healing

Posted Date: March 13th, 2021

DOI: https://doi.org/10.21203/rs.3.rs-286190/v1

Abstract

Development of incisional hernia (IH) is multifactorial but inflammation and abdominal wall ECM (extracellular matrix) disorganization are key pathological events. We investigated if the differential expression of fibroblast biomarkers reflects the cellular milieu and the dysregulated ECM in IH tissues. Expression of fibroblast biomarkers, including connective tissue growth factor, alpha-smooth muscle actin (α-SMA), CD34 (cluster of differentiation 34), cadherin-11 and fibroblast specific protein 1 (FSP1), was examined by histology and immunofluorescence in the hernial-fascial ring/neck tissue (HRT) and hernia sack tissue (HST) harvested from the patients undergoing hernia surgery and compared with normal fascia (FT) and peritoneum (PT) harvested from brain-dead healthy subjects undergoing organ procurement for transplantation. The H&E staining revealed alterations in tissue architecture, fibroblast morphology, and ECM organization in the IH tissues compared to control. The biomarker for undifferentiated fibroblasts, CD34, was significantly higher in HST and decreased in HRT than the respective FT and PT controls. Also, the findings revealed an increased level of CTGF (connective tissue growth factor) with decrease in α-SMA in both HRT and HST compared to the controls. In addition, an increased level of FSP1 (fibroblast specific protein 1) and cadherin-11 in HRT with decreased level in HST were observed relative to the respective controls (FT and PT). Hence, these findings support the heterogeneity of fibroblast population at the laparotomy site that could contribute to the development of IH. Understanding the mechanisms causing the phenotype switch of these fibroblasts would open novel strategies to prevent the development of IH following laparotomy.

Introduction

The incidence of IH following a laparotomy is on average reported to be between 10–20% but is much higher (up to 30%) in certain subpopulations such as those undergoing a colectomy for diverticulitis [1] [2]. The development of an incisional hernia (IH) following a laparotomy is the result of many factors and associated comorbid conditions but inflammation and disorganization of abdominal wall extracellular matrix (ECM) aggravate the pathology and undoubtedly play a significant role [3]. An incomplete healing response following an abdominal incision impedes the restoration of abdominal wall ECM which fails to perform the load-bearing functions at the myofascial layer [4]. Alterations in connective tissue metabolism especially the collagenopathies has gained significance in IH pathology, as the histology of the IH tissues are characterized by drastic ECM disorganization [3] [5]. The biochemical pathology of IH formation reveals the derangements in the expression of collagen subtypes and dysregulation of matrix metalloproteinases (MMPs). The decreased ratio of collagen I/III and the hyperactivity of various MMPs lead to weak ECM which in turn paves way to IH formation [6].

The abdominal wall fascia, a fibrous tissue which provides physical support to abdominal muscles, has been considered a most important tissue in hernia formation [7] [8]. The highly organized ECM of fascia is primarily maintained by the resident fibroblasts. The ECM homeostasis depends on the phenotypic stability of the fibroblasts in which several extrinsic and/or intrinsic factors influence the physiological functions of these fibroblasts in the fascial tissue [9]. Moreover, the structural and functional integrity of

the fascia largely depends on the quality of ECM, where the alterations in the phenotype of these fibroblasts following a laparotomy result in impaired ECM and delayed repair response [9]. Following a tissue insult, the resident fibroblasts acquire a contractile phenotype, the myofibroblasts, resulting in ECM deposition to accelerate the process of tissue repair [10]. However, limited information is available regarding the phenotype of fibroblasts in the IH tissues.

There is a paucity of available literature to define the phenotype and distribution of the fibroblasts present in IH tissue. However, mature fibroblasts in other tissues are negative for α-smooth muscle actin (α-SMA) [11]. On the other hand, the α-SMA-positive proliferative myofibroblasts represent ECM repair in the damaged tissue which eventually undergo apoptosis once a functional ECM is re-established [12]. Moreover, the normal fibroblasts are characterized by the expression of biomarkers such as podoplanin, cadherin-11, CD34, and fibroblast specific protein − 1 (FSP1) [13]. In addition, the connective tissue growth factor (CTGF) secreted by the fibroblasts stimulates ECM production by promoting cell adhesion, migration and differentiation [14]. Since the level of CTGF is high during early phase of wound healing, the degree of CTGF release signifies the stage of wound healing [15]. Hence, the expression status of the cellular biomarkers including cadherin-11, CD34, and FSP1, fibroblast-derived ECM homeostasis regulatory signal CTGF, and the wound healing fibroblast biomarker α-SMA would define the fibroblasts associated with the pathology of IH. However, the phenotypes of fibroblast cells in the IH tissues based on the expression of these biomarkers are largely undefined. Based on this background, we hypothesize that the expression level of fibroblast biomarkers reflects the cellular milieu and the dysregulated ECM in IH tissues. Hence, the present study was designed to examine the expression of different fibroblast biomarkers in the IH tissues of the fascial ring and hernia sac harvested from patients undergoing incisional hernia repair and compared with the normal controls of fascial tissue (FT) and peritoneal tissue (PT), respectively.

Materials And Methods

Tissue harvest and processing

Institutional Review Board (IRB) of Creighton University approved the study under the IRB protocol (2nd May 2018 to 2nd April 2019) of Robert J. Fitzgibbons, MD, a co-author of this article.
All methods were performed in accordance with the relevant guidelines and regulations.
Patients ≥ 19 years of age, of either sex, who were undergoing repair of incisional hernia were recruited in the study and informed consent were obtained. The patients presented for hernias other than IH and patients without laparoscopy were excluded in the study. All signed consent forms and HIPPA forms are saved in the office of Robert J. Fitzgibbons, MD.
The surgical waste tissues for the experiments were obtained from 10 patients who underwent hernia repair.
The de-identified tissues were sent to the laboratory for further experiments.

The hernial-fascial ring/neck tissue (HRT) and the hernia sack tissue (HST) were collected (Fig. 1) in the commercially available UW (*University of Wisconsin*) solution for transportation to research laboratory and used within 24 hours. The composition of the UW solution included: 50g/L pentafraction, 35.83g/L lactobionic Acid (as Lactone), 3.4g/L potassium phosphate monobasic, 1.23g/L magnesium sulfate heptahydrate, 17.83g/L raffinose pentahydrate, 1.34g/L adenosine, 0.136g/L allopurinol, 0.922g/L total glutathione, 5.61g/L potassium hydroxide, and pH 7.4. The tissue specimens were then fixed in formalin, embedded in paraffin wax, and sections of 5μm thickness were taken using microtome (Leica, Germany) for histology and immunofluorescence analysis. Abdominal wall fascial tissue (FT) was used as control for HRT and the peritoneal tissue (PT) was used as control for HST.

The FT and PT were provided by Live On Nebraska (formerly called Nebraska Organ Recovery System) as control tissues from 5 registered organ donors at the time of organ harvest.
The approval for collecting such tissues was also obtained under the approved IRB protocol of Robert J. Fitzgibbons, MD, a co-author of this article. The control tissues were harvested from the abdominal wall at the time of laparotomy to harvest intra-abdominal organs. The control tissues were also processed in the same manner as the hernia patient tissues. Adjacent sections from each specimen were utilized for all examination to ensure similar histomorphology.

H&E staining

The tissue sections were deparaffinized and used for H&E staining to examine the tissue morphology and ECM organization following a previously reported protocol [16] [17]. After staining, the slides were imaged using a slide scanner system (VS120-S6-W, Olympus) at 20x magnification and the images were converted to JPEG format using OlyVIA Desktop software. The images were examined qualitatively to evaluate the alteration in histology and were compared with the controls.

Immunofluorescence

The protein expression of biomarkers to identify the cell phenotypes in the tissue sections was analyzed by immunofluorescence following the protocols standardized in our laboratory [16] [17]. Briefly, antigen retrieval was performed in the tissue by warming at 95^{o}C for 20 min in HIER buffer (Heat Induced Antigen Retrieval; TA-135-HBM) followed by blocking with 0.25 % Triton X-100 and 5% horse serum in PBS at room temperature for 2 hrs. Primary antibodies against CTGF (ab5097), α-SMA (ab5694), CD34 (ab81289), cadherin-11 (ab151302) and FSP1 (ab197896) were purchased from Abcam and used in a dilution of 1:300 in the tissue sections and incubated overnight at 4^{o}C. Corresponding fluorochrome-conjugated secondary antibody, donkey anti-rabbit-594 (A21207, ThermoFisher Scientific) was used in a dilution of 1:300 to bind the primary antibody. A negative control with secondary antibody alone was maintained in a similar manner to detect background fluorescence and optimize the exposure time. Nuclei were counterstained with 4',6-diamidino-2-phenylindole (DAPI) (H-1200) and the images were acquired using a fluorescent slide scanner system (VS120-S6-W, Olympus) at 20x magnification and the images were taken and converted to JPEG format using OlyVIA Desktop software. The fluorescence intensity was quantified using ImageJ software and the results are expressed as mean fluorescence

intensity (MFI). For MFI quantification 3–4 images were randomly acquired from each specimen and were averaged for each specimen. Also, the blood vessels contained in the tissue specimen were included for MFI quantification. The MFI values per 100 cells were normalized and compared with the control. In order to ensure consistency in data analysis, brightness value was kept in the range of 40–50 and the threshold value was kept in the range of 70–80 for cell count during background clearance using ImageJ. The values of MFI/100 cells were used to calculate the variation with respect to the control (ratio of respective MFI/100 cells of the specimen to that of average control) which in turn was represented as fold-change expression calculated by transforming to logarithmic (Log_2) scale.

Statistical analysis

The results of MFI for FT (n = 5), PT (n = 4), HRT (n = 10) and HST (n = 10) were expressed as mean ± SEM. Also, the specimens that persistently displayed folding and background fluorescence were omitted from statistical analysis. The statistical significance was assessed by unpaired one-way ANOVA with Tukey's multiple comparison test using GraphPad Prism software. The intensity of each tissue specimen corresponds to the average MFI of 3–4 images acquired randomly from different fields. The average MFI of individual specimen was used to calculate the % variation (by normalizing 100% for controls) followed by fold change expression which, in turn, was used to calculate the average mean and SEM for statistical analysis. The $p < 0.05$ values were considered to be significant in all experiments.

Results

Histomorphology

Figure 1 displays the anatomical sites of HST and HRT harvest. The H&E staining displayed alterations in tissue architecture, fibroblast morphology, and ECM organization in the IH tissues when compared with controls (Fig. 2). The control groups exhibited undamaged and well-organized ECM with mature and inactive fibroblasts as evident from their elongated nuclei surrounded by an intact matrix. On the other hand, the HRT and HST displayed the pathological features such as highly disorganized ECM, infiltration of adipose tissue, blood vessel formation and inflammation. White blood cells (WBCs) were observed in HRT and HST as identified by their characteristic nuclei. The localized inflammation was characterized by the presence of neutrophils and monocytes. Oval nuclear morphology of the cells displayed by HRT and HST represents proliferative fibroblasts. These pathological features were completely absent in the control tissues.

Protein expression of biomarkers

Protein expression of the biomarkers is represented as fold change with respective to the corresponding controls. The fold-change was calculated from MFI normalized with the total number of cells based on nuclei count in each microscopic field.

The average MFI/cell obtained from the control group for each biomarker was normalized with corresponding MFI/cell values obtained from individual HST and HRT specimen to calculate the variation with respect to the control (VRC).

The fold-change represents the log2 values of VRC. The level of FSP1 was increased in HRT and decreased in HST when compared to FT and PT, respectively; however, the change was statistically not significant (Figs. 3A and 6). Cadherin-11 expression was significantly increased in HRT when compared to FT and was decreased in HST than PT; however, the decrease was statistically not significant (Fig. 3B and 6). The protein expression of CD34, the biomarker for undifferentiated fibroblasts, was significantly higher in HST and was decreased in a statistically non-significant manner in HRT than the corresponding controls (Figs. 4A and 6). The α-SMA, the biomarker for myofibroblasts, was decreased in HRT and HST when compared to the respective controls, FT, and PT; however, the decrease was statistically not significant (Figs. 4B and 6). Also, the α-SMA expression was mostly found in the blood vessels of the controls (FT and PT) whereas in HRT and HST the α-SMA expression was confined in both blood vessels and tissue. The protein expression of CTGF, the secretory protein by fibroblasts, was significantly higher in HRT and HST compared to respective controls (Figs. 5 and 6). The protein expression of FSP1, and cadherin-11 were significantly higher in HRT when compared to HST; CD34 was significantly higher in HST than HRT; and the change in other biomarkers was not statistically significant between the HST and HRT. In addition, the control specimen exhibited variability within the group and the variability among the control specimen are displayed in Fig. 6B. The values for the fold change in each biomarker with respect to the corresponding controls and the P values for statistical significance are displayed in Table 1.

Table 1
The fold change expression of the biomarkers calculated from the MFI (mean fluorescence intensity) values relative to control and the respective P values

Biomarkers	HST (FT)	PT vs HST	HRT (FT)	PT vs HRT	HRT vs HST
FSP1 (Fibroblast specific Protein 1)	-0.43 ± 0.23	*P = 0.3306*	0.23 ± 0.17	*P = 0.5202*	*P = 0.0472*
Cadherin-11	-0.82 ± 0.31	*P = 0.1332*	2.42 ± 0.20	*P < 0.0001*	*P < 0.0001*
CD34 (Cluster of differentiation 34)	2.09 ± 0.27	*P < 0.0001*	-0.006 ± 0.23	*P = 0.9999*	*P < 0.0001*
α-SMA (Alpha-smooth muscle actin)	-0.067 ± 0.28	*P = 0.9898*	-1.05 ± 0.0994	*P = 0.5781*	*P = 0.0527*
CTGF (Connective tissue growth factor)	1.69 ± 0.46	*P = 0.0364*	1.71 ± 0.34	*P = 0.0332*	*P = 0.9984*

FT, fascial tissue ; HRT, hernial-fascial ring/neck tissue ; HST, hernia sack tissue ; PT, peritoneal tissue.

Discussion

IH occurs as a result of fascial tissue deficiency due to impairment in surgical wound healing following a laparotomy [18]. Pathological evaluation of tissue from IH patients discloses cellular and extracellular derangements in the abdominal wall tissue [19]. Disturbance in collagen homeostasis has been previously incriminated in the development of IH. Our study supports the concept that abnormal/altered fibroblast population results in the synthesis of abnormal ECM components leading to the development of IH following a laparotomy [13]. The exact mechanism of the selection of altered fibroblast phenotypes is unknown; however, it is believed that the loss of mechanical integrity of abdominal wall due to the incision somehow signals the fibroblasts to attain a pathological phenotype resulting in defective collagen production [19] [20]. Since the tissue fibroblasts are associated with ECM homeostasis, alterations in the fibroblast phenotypes signify a possible mechanism underlying IH formation. The identification and characterization of pathological fibroblasts in the IH tissues should pave the way for a better understanding the IH pathology.

In this study, the histological architecture of the hernia tissues was altered considerably when compared with the control suggesting that the persistence of ECM disorganization is involved in IH pathology. A shift in nuclear morphology from linear to oval shape was observed in fibroblast cells of IH tissues signifying the existence of altered phenotypes. It has been reported that the oval, spindle and/or stellate shaped cells with round or oval nuclei represent active (proliferative) fibroblasts which reflect ECM pathology [21]. Based on the nuclear morphology, the proliferative fibroblasts were predominant in HRT and HST. On the other hand, the control tissues displayed elongated wavy nuclei representing mature/inactive fibroblasts which were surrounded by intact ECM [21] [22]. Moreover, the fibroblasts exist in the tissues as heterogeneous phenotypes with various subpopulations having distinct functions other than ECM homeostasis such as immune accessory cells, wound healing, inflammation and tissue regeneration [21].

The current strategies are limited to define the heterogeneity of fibroblasts under physiological and pathological conditions and to understand their complex role in IH pathology. Our approach was to examine and compare the fibroblast phenotypes by assessing the expression of fibroblast specific biomarkers in IH and normal abdominal wall tissues. The FSP1 (also known as S100A4 and is a specific biomarker for fibroblasts) has a significant role in regulating epithelial to mesenchymal transition, apart from its role in fibrosis [23] [24] [25]. The increased expression of FSP1 in HST can be correlated with fatty infiltration as observed by histology. The increased expression of FSP1 with concomitantly increased adipose tissue infiltration suggesting the possible role of fibroblasts as adipocyte precursor. However, further investigations are warranted to validate the adipogenic function of fibroblasts in the IH tissues.

CD34 is a transmembrane glycoprotein which marks hematopoietic progenitor cells and mesenchymal stem cells (MSCs) [26]. As the expression of CD34 was confined to extravascular tissues, the possibility of endothelial cell lineages is minimal in the studied specimen. Also, CD34 is a biomarker for undifferentiated fibroblasts that are critical in tissue remodeling [27]. Since MSCs and fibroblasts share mesenchymal origin and specific biomarkers, further characterization are warranted to distinguish these

cell population. The progressive loss of CD34 paves the way in the induction of α-SMA + myofibroblasts [28]. CD34 + cells were increased in HST when compared to the control, which was in accordance with the histological findings. This suggests that the proliferation of undifferentiated fibroblasts is an obstacle in the trans-differentiation of myofibroblasts resulting in abnormal wound healing. Also, the undifferentiated fibroblasts secrete incomplete ECM and result in disorganization as evident in the histology [21]. The similar expression profile of CD34 in HRT and FT reveals the presence of matured tissue suggesting that the IH pathology nucleates at HST by depositing abnormal ECM which eventually leads to form IH in an unknown mechanism and warrants further investigation.

The α-SMA has been considered to be a pivotal biomarker for myofibroblasts, which are contractile phenotype of fibroblasts mainly associated with wound healing response; especially in the process of wound contraction [29] [30]. The decreased expression of α-SMA in the HST and HRT shows the impaired wound healing phase or wound progression suggesting the persistence of pathology or dysfunction of myofibroblasts. Moreover, the correlation of α-SMA with the status of wound healing and severity of IH pathology is warranted deciphering its role in IH formation. Moreover, multiple cell phenotypes including vascular smooth muscle cells, pericytes and fibroblasts express α-SMA and we performed quantification of the fluorescence intensity for total α-SMA. In addition, the blood vessels in tissue sections displayed upregulation of α-SMA; however, the exclusion of blood vessels from the analysis was difficult owing to their increased density. Interestingly, extra vascular tissues displayed the immunopositivity for α-SMA suggesting the α-SMA-positive fibroblast phenotypes as predominantly evident in HST and HRT which provides qualitative understanding regarding the expression status in α-SMA extra vascular tissues. However, co-staining with extravascular biomarkers is warranted to distinguish fibroblasts from cells of vascular lineage. Based on these observations, it is logical that the trans-differentiation signaling of fibroblasts to myofibroblasts is impaired in HRT tissues resulting in abnormal wound healing and IH formation. However, the exact mechanisms underlying the trans-differentiation of myofibroblasts in IH tissues are unknown and warrant further investigation.

CTGF has been identified as a fibrogenic factor which co-expresses with transforming growth factor-β (TGF-β) and triggers fibroblast proliferation, migration, and ECM synthesis. Basal level of CTGF expression has been reported in normal tissues whereas CTGF level increases in the fibrotic tissues [31]. Reactive oxygen species (ROS) and oxidative stress are well known triggers for CTGF expression; however the involvement of ROS in IH pathology has not been studied [32] [33]. Even though the actual role of CTGF in IH pathology is not clear the increased levels of CTGF in HRT and HST suggest a healing response elicited by the surviving tissue. However, CTGF-silenced animal models of IH could be helpful to elucidate the mechanism of CTGF action in IH pathology.Cadherin-11 is engaged in the release of pro-inflammatory signals such as IL-6, TNF-α and IL-1β from the fibroblasts of injured tissues [34] [35]. In addition, cadherin-11 is associated with the expression of various ECM components including collagen and elastin and regulates the mechanical integrity of the tissue and wound healing responses[36]. Despite significant upregulation of cadherin-11 in HRT and HST, the functional role of cadherin-11 in the inflammation and ECM damage associated with IH are largely unknown and requires more attention.

The present study focused on the examination of the expression of biomarkers of fibroblasts and to define their phenotypes based on their expression in IH. The biomarkers chosen for the current study were based on their characteristic expression on fibroblast subpopulations and displayed considerable alterations between HRT and HST and the respective controls FT and PT suggesting a possible association with IH pathology. However, the expression status of these biomarkers has not been established in post-laparotomy IH formation which requires further research to unveil the molecular events leading to IH formation. Moreover, the information regarding the characterization of abnormal fibroblast population in IH tissues based on these biomarkers is unavailable. To our knowledge, this is the first study focusing on phenotyping fibroblast in IH formation and the overall findings are displayed in Fig. 7. Our major findings revealed differential expression of these biomarkers in HST and HRT (the major susceptible sites for IH formation) suggesting the existence of diverse fibroblast phenotypes in these tissues which in turn reflects the difference in molecular pathology. However, the exact molecular mechanism underlying the regulation of diverse fibroblast phenotypes based on the biomarker expression warrants further investigation.

The present study has several limitations including the unavailability of specific biomarker for fibroblasts that limits the co-localization studies. Moreover, the specificity of the biomarkers is questionable since they might be expressed in other cell types including immune cells and stem cells. Hence, proper definition of IH fibroblasts based on specific biomarker panel is warranted. In addition, the cellular composition in HST and HRT has not been established and the phenotype of extra fibroblasts warrants further attention. Other limitations include the lack of co-expression studies of the biomarkers with other cell types such as MSCs, smaller size of control tissues, relatively small number of patient/control tissue specimen, variability among the patients and controls, and lack of *in vitro* validation. Due to the limited availability of control specimen and smaller size of specimen, it was not possible to perform PCR and western blot analysis. However, the present study utilized MFI-based semi-quantitative fold-change to represent the expression status of biomarkers. In addition, the present study mainly relied on the immunopathology and further investigation based on proteomics, genomics and metabolomics are warranted. Nevertheless, the findings from this study strongly suggest that the heterogeneity of the fibroblast population could play a critical role in the development of IH. Understanding the mechanism underlying the phenotype switch of these fibroblasts would open opportunities to develop novel strategies to prevent the development of IH following a laparotomy.

Conclusion

The IH tissues displayed considerable histological alterations such as ECM disorganization, fatty infiltration and inflammation when compared with the control tissue.

The findings revealed increased level of CTGF and, decreased α-SMA in both HRT and HST, increased FSP1 and cadherin-11 in HRT with decreased levels in HRT, and decreased CD-34 in HRT and increased level in HST relative to the respective controls FT and PT, suggesting alterations in fibroblast phenotypes and the possible association of these altered fibroblast phenotypes in the IH pathology (Fig.

8). These findings open up the opportunities to further define the heterogeneity in fibroblast population and to investigate the underlying mechanism of their phenotype switch to develop better management strategies in patients undergoing a laparotomy.

Declarations

The authors report no proprietary or commercial interest in any product mentioned or concept discussed in this article.

Funding: This research work was supported by NIH-NHLBI grants R01HL147662 and R01HL144125 of DK Agrawal and CU Surgery research funds to Dr. Fitzgibbons. The content of this original article is solely the responsibility of the authors and does not necessarily represent the official views of the NIH.

Conflicts of interest/Competing interests: The authors declare no conflict of interest.

Ethics approval: Institutional Review Board (IRB) of Creighton University approved the study under the IRB protocol (2nd May 2018 to 2nd April 2019) of Robert J. Fitzgibbons, MD, a co-author of this article.

Consent to participate: Patients ≥19 years of age, of either sex, who were undergoing repair of their incisional hernia were recruited in the study and informed consents and HIPPA forms were obtained and saved in the office of Robert J. Fitzgibbons, MD. The de-identified tissues were sent to the laboratory for further experiments.

Consent for publication: There is no identifiable images or other personal or clinical details of study participants in the data presented. As the corresponding authors, I verify that all authors significantly contributed in various aspect of the study, have read the manuscript and consented to submit for publication in the *Molecular and cellular biochemistry.*

Availability of data and material (data transparency): There is no restrictions on sharing a de-identified data set (without any identifying or sensitive patient information) on the experiments performed on the human tissues collected and processed in an un-identifiable manner. Such data are now included as Supporting Information Excel file. This file contains: (i) the values behind the means, standard deviations and other measures reported, and (ii) the values used to build graphs.

Code availability (software application or custom code): Not applicable

Authors' Contribution: Conception and design: FGT, NKL, RJF, DKA; Contributed reagents/ materials/analysis tool: RJF, DKA; Conducting surgeries, analysis and interpretation of the data: RJF, NKL, FGT, AV, T-NB, MR, DKA; Drafting of the article: FGT, NKL, DKA; Critical revision and editing of the article for important intellectual content: FGT, NKL, RJF, DKA; Final approval of the submitted article: FGT, NKL, AV, T-NB, MR, RJF, DKA.

Acknowledgement: The authors would like to sincerely acknowledge the staffs of Live on Nebraska (Formerly called NORS (Nebraska Organ Recovery System) for procuring control specimen in this study.

References

1. Reistrup H, Zetner DB, Andresen K, Rosenberg J (2018) [Prevention of incisional hernia]. Ugeskr Laeger 180
2. Deng Y, Ren J, Chen G et al (2017) Injectable in situ cross-linking chitosan-hyaluronic acid based hydrogels for abdominal tissue regeneration. Sci Rep 7:. https://doi.org/10.1038/s41598-017-02962-z
3. Harrison B, Sanniec K, Janis JE (2016) Collagenopathies—Implications for Abdominal Wall Reconstruction: A Systematic Review. Plast Reconstr Surg - Glob Open 4:e1036. https://doi.org/10.1097/GOX.0000000000001036
4. Guillen-Marti J, Diaz R, Quiles MT et al (2009) MMPs/TIMPs and inflammatory signalling de-regulation in human incisional hernia tissues. J Cell Mol Med 13:4432–4443. https://doi.org/10.1111/j.1582-4934.2008.00637.x
5. Henriksen NA, Yadete DH, Sorensen LT et al (2011) Connective tissue alteration in abdominal wall hernia. Br J Surg 98:210–219. https://doi.org/10.1002/bjs.7339
6. Yahchouchy-Chouillard E, Aura T, Picone O et al (2003) Incisional Hernias. Dig Surg 20:3–9. https://doi.org/10.1159/000068850
7. Ireton JE, Unger JG, Rohrich RJ (2013) The role of wound healing and its everyday application in plastic surgery: a practical perspective and systematic review. Plast Reconstr Surg Glob Open 1:. https://doi.org/10.1097/GOX.0b013e31828ff9f4
8. Rath AM, Chevrel JP (1998) The healing of laparotomies: review of the literature: Part 1. Physiologic and pathologic aspects. Hernia 2:145–149. https://doi.org/10.1007/BF01250034
9. Diaz R, Quiles MT, Guillem-Marti J et al (2011) Apoptosis-Like Cell Death Induction and Aberrant Fibroblast Properties in Human Incisional Hernia Fascia. Am J Pathol 178:2641–2653. https://doi.org/10.1016/j.ajpath.2011.02.044
10. Dobaczewski M, Gonzalez-Quesada C, Frangogiannis NG (2010) The extracellular matrix as a modulator of the inflammatory and reparative response following myocardial infarction. J Mol Cell Cardiol 48:504–511. https://doi.org/10.1016/j.yjmcc.2009.07.015
11. Frangogiannis NG (2016) Fibroblast—Extracellular Matrix Interactions in Tissue Fibrosis. Curr Pathobiol Rep 4:11–18. https://doi.org/10.1007/s40139-016-0099-1
12. Li B, Wang JH-C (2011) Fibroblasts and myofibroblasts in wound healing: Force generation and measurement. J Tissue Viability 20:108–120. https://doi.org/10.1016/j.jtv.2009.11.004
13. Thankam FG, Palanikumar G, Fitzgibbons RJ, Agrawal DK (2019) Molecular Mechanisms and Potential Therapeutic Targets in Incisional Hernia. J Surg Res 236:134–143. https://doi.org/10.1016/j.jss.2018.11.037

14. Henshaw FR, Boughton P, Lo L et al (2015) Topically Applied Connective Tissue Growth Factor/CCN2 Improves Diabetic Preclinical Cutaneous Wound Healing: Potential Role for CTGF in Human Diabetic Foot Ulcer Healing. J Diabetes Res 2015:1–10. https://doi.org/10.1155/2015/236238
15. Alfaro MP, Deskins DL, Wallus M et al (2013) A physiological role for connective tissue growth factor in early wound healing. Lab Invest 93:81–95. https://doi.org/10.1038/labinvest.2012.162
16. Thankam FG, Boosani CS, Dilisio MF et al (2016) MicroRNAs Associated with Shoulder Tendon Matrisome Disorganization in Glenohumeral Arthritis. PLOS ONE 11:e0168077. https://doi.org/10.1371/journal.pone.0168077
17. Thankam FG, Dilisio MF, Dietz NE, Agrawal DK (2016) TREM-1, HMGB1 and RAGE in the Shoulder Tendon: Dual Mechanisms for Inflammation Based on the Coincidence of Glenohumeral Arthritis. PLOS ONE 11:e0165492. https://doi.org/10.1371/journal.pone.0165492
18. Xing L, Culbertson EJ, Wen Y, Franz MG (2013) Early laparotomy wound failure as the mechanism for incisional hernia formation. J Surg Res 182:e35–e42. https://doi.org/10.1016/j.jss.2012.09.009
19. Franz MG (2008) The Biology of Hernia Formation. Surg Clin North Am 88:1–15. https://doi.org/10.1016/j.suc.2007.10.007
20. Benjamin M, Hillen B (2003) Mechanical Influences on Cells, Tissues and Organs ? ?Mechanical Morphogenesis? Eur J Morphol 41:3–7. https://doi.org/10.1076/ejom.41.1.3.28102
21. Ravikanth M, Manjunath K, Ramachandran C et al (2011) Heterogenecity of fibroblasts. J Oral Maxillofac Pathol 15:247. https://doi.org/10.4103/0973-029X.84516
22. Lekic PC, Pender N, McCulloch CA (1997) Is fibroblast heterogeneity relevant to the health, diseases, and treatments of periodontal tissues? Crit Rev Oral Biol Med Off Publ Am Assoc Oral Biol 8:253–268
23. Kong P, Christia P, Saxena A et al (2013) Lack of specificity of fibroblast-specific protein 1 in cardiac remodeling and fibrosis. Am J Physiol-Heart Circ Physiol 305:H1363–H1372. https://doi.org/10.1152/ajpheart.00395.2013
24. Strutz F, Okada H, Lo CW et al (1995) Identification and characterization of a fibroblast marker: FSP1. J Cell Biol 130:393–405
25. Zhang R, Gao Y, Zhao X et al (2018) FSP1-positive fibroblasts are adipogenic niche and regulate adipose homeostasis. PLOS Biol 16:e2001493. https://doi.org/10.1371/journal.pbio.2001493
26. Sudheer Shenoy P, Bose B (2017) Identification, isolation, quantification and systems approach towards CD34, a biomarker present in the progenitor/stem cells from diverse lineages. Methods 131:147–156. https://doi.org/10.1016/j.ymeth.2017.06.035
27. Silverman JS, Tamsen A (1998) CD34 and factor XIIIa-positive microvascular dendritic cells and the family of fibrohistiocytic mesenchymal tumors. Am J Dermatopathol 20:533–536
28. San Martin R, Barron DA, Tuxhorn JA et al (2014) Recruitment of CD34(+) fibroblasts in tumor-associated reactive stroma: the reactive microvasculature hypothesis. Am J Pathol 184:1860–1870. https://doi.org/10.1016/j.ajpath.2014.02.021

29. Van De Water L, Varney S, Tomasek JJ (2013) Mechanoregulation of the Myofibroblast in Wound Contraction, Scarring, and Fibrosis: Opportunities for New Therapeutic Intervention. Adv Wound Care 2:122–141. https://doi.org/10.1089/wound.2012.0393
30. Micallef L, Vedrenne N, Billet F et al (2012) The myofibroblast, multiple origins for major roles in normal and pathological tissue repair. Fibrogenesis Tissue Repair 5:S5. https://doi.org/10.1186/1755-1536-5-S1-S5
31. Yang Z, Sun Z, Liu H et al (2015) Connective tissue growth factor stimulates the proliferation, migration and differentiation of lung fibroblasts during paraquat-induced pulmonary fibrosis. Mol Med Rep 12:1091–1097. https://doi.org/10.3892/mmr.2015.3537
32. Tsai C-C, Wu S-B, Chang P-C, Wei Y-H (2015) Alteration of Connective Tissue Growth Factor (CTGF) Expression in Orbital Fibroblasts from Patients with Graves' Ophthalmopathy. PLOS ONE 10:e0143514. https://doi.org/10.1371/journal.pone.0143514
33. Lee CH, Shah B, Moioli EK, Mao JJ (2010) CTGF directs fibroblast differentiation from human mesenchymal stem/stromal cells and defines connective tissue healing in a rodent injury model. J Clin Invest 120:3340–3349. https://doi.org/10.1172/JCI43230
34. Chang SK, Noss EH, Chen M et al (2011) Cadherin-11 regulates fibroblast inflammation. Proc Natl Acad Sci 108:8402–8407. https://doi.org/10.1073/pnas.1019437108
35. Schroer A, Bersi M, Clark C et al (2019) CADHERIN-11 BLOCKADE REDUCES INFLAMMATION DRIVEN FIBROTIC REMODELING AND IMPROVES OUTCOMES AFTER MYOCARDIAL INFARCTION: Compiled Supplmental Methods and Figures. bioRxiv. https://doi.org/10.1101/533000
36. Row S, Liu Y, Alimperti S et al (2016) Cadherin-11 is a novel regulator of extracellular matrix synthesis and tissue mechanics. J Cell Sci 129:2950–2961. https://doi.org/10.1242/jcs.183772

Figures

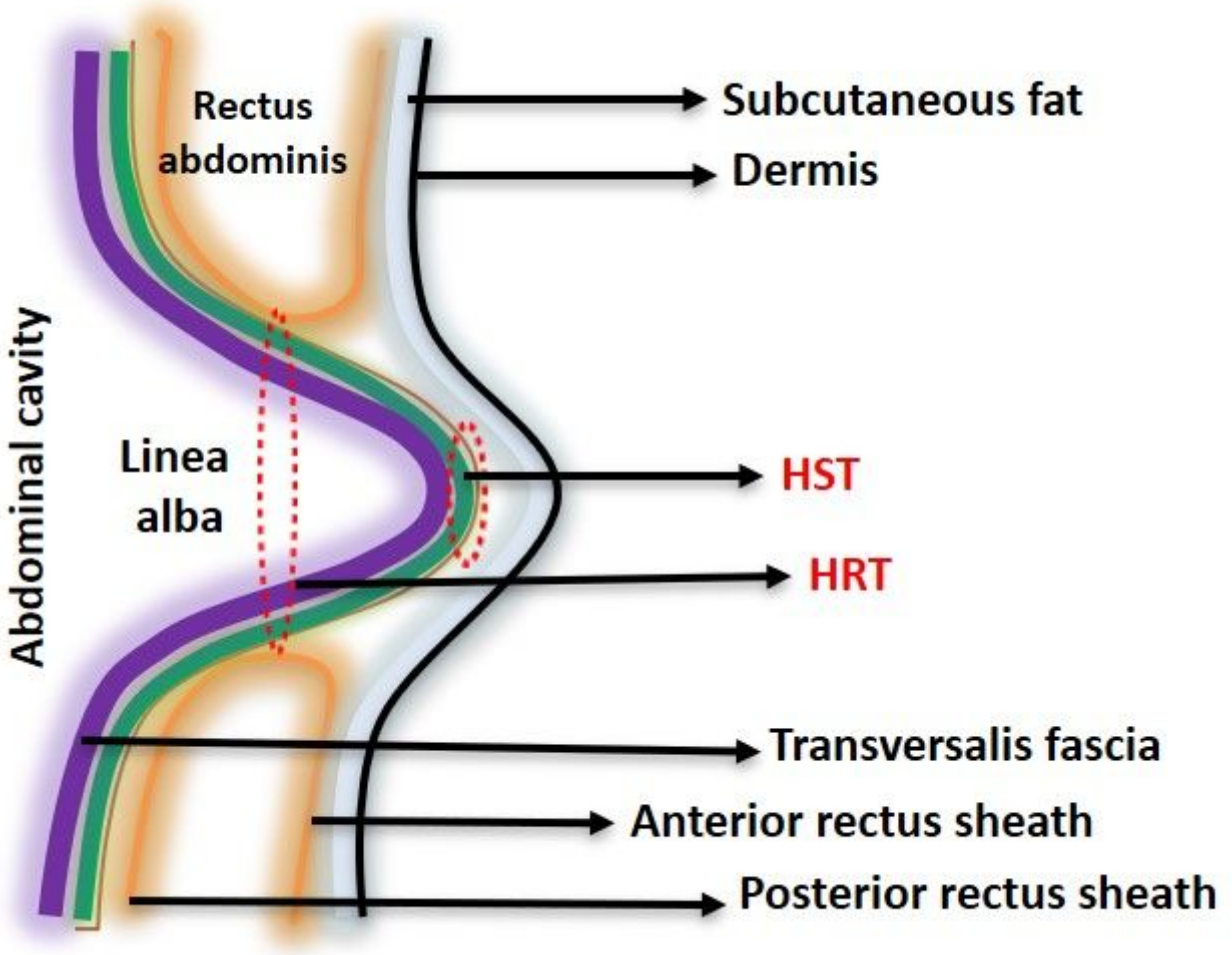

Figure 1

Schematic representation for the anatomical location of harvesting HST, HRT and control specimen. The illustration depicts where the analyzed tissue biopsies for hernial-fascial ring/neck tissue (HRT) and the hernia sack tissue (HST) were collected and used in this study.

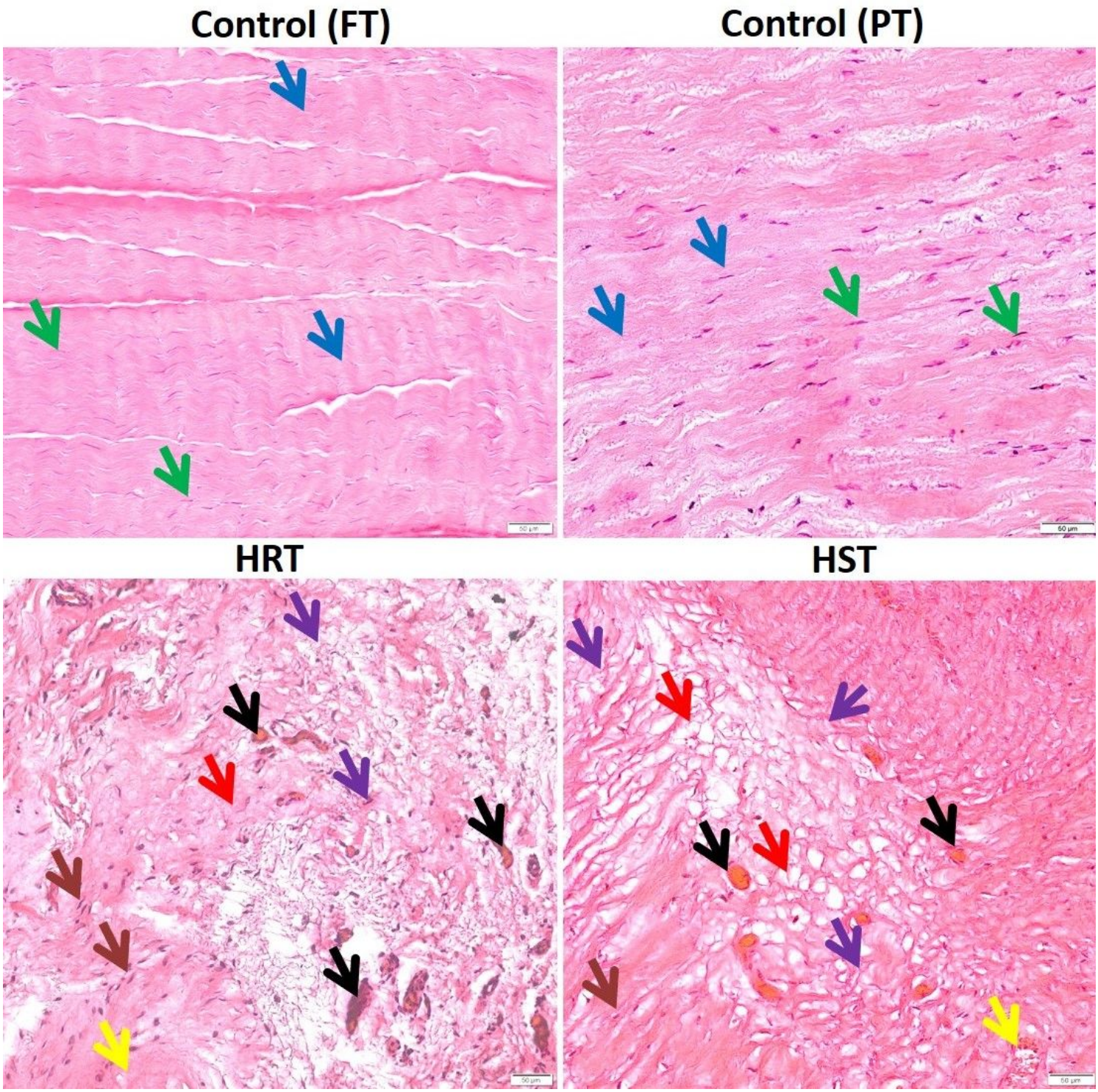

Figure 2

Histomorphology examination by H&E staining: Representative images of H&E staining for controls (FT and PT), HRT and HST revealed the extent of ECM organization/disorganization. The green arrows show mature fibroblasts, the brown arrows display proliferative fibroblasts, blue arrows point intact ECM, purple arrows indicate ECM disorganization, red arrows point fatty infiltration, black arrow indicate angiogenesis and yellow arrows reveal inflammation. The control group image represents abdominal wall tissue (N=5)

and the other groups HRT and HST represent 10 patients each. The images were acquired in 20x magnification (Scale bar - 50µm).

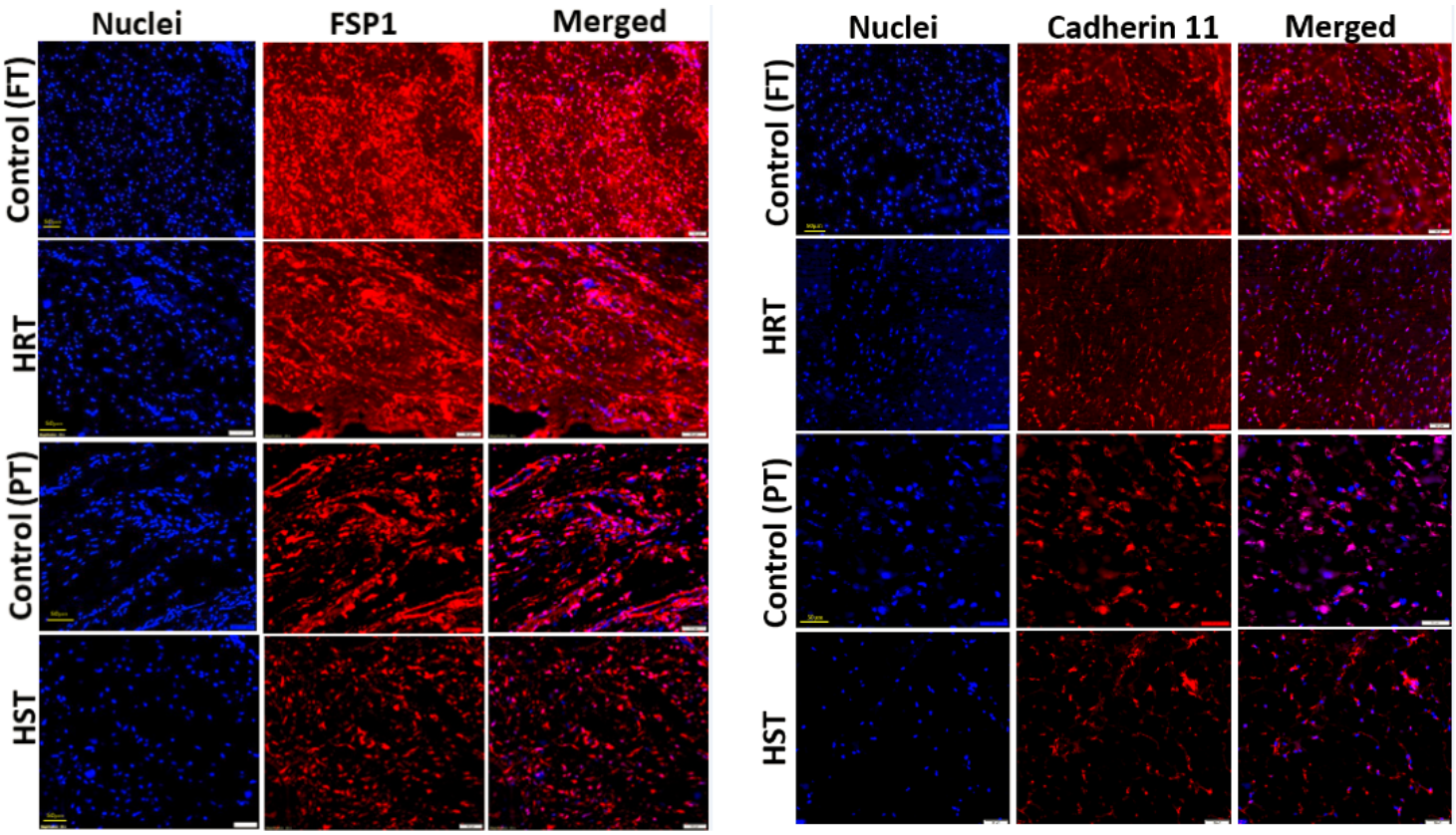

Figure 3

Representative images of the immunofluorescence analysis for the protein expression of FSP1 (3A) and Cadherin-11 (3B) of HRT and HST with comparison to controls (FT and PT): Images in the left column show nuclear staining with DAPI; the images in the middle column show expression of the respective biomarker while the images in the right column show overlay of the biomarker staining with DAPI. Images were acquired at 20x magnification (Scale bar -50µm) using CCD camera attached to the Olympus slide scanner microscope. In FSP1 analysis, n=4 for FT, n=3 for PT, n=8 for HST and n=10 for HRT and in Cadherin-11 analysis, n=5 for FT, n=4 for PT, n=10 for HST and n=10 for HRT.

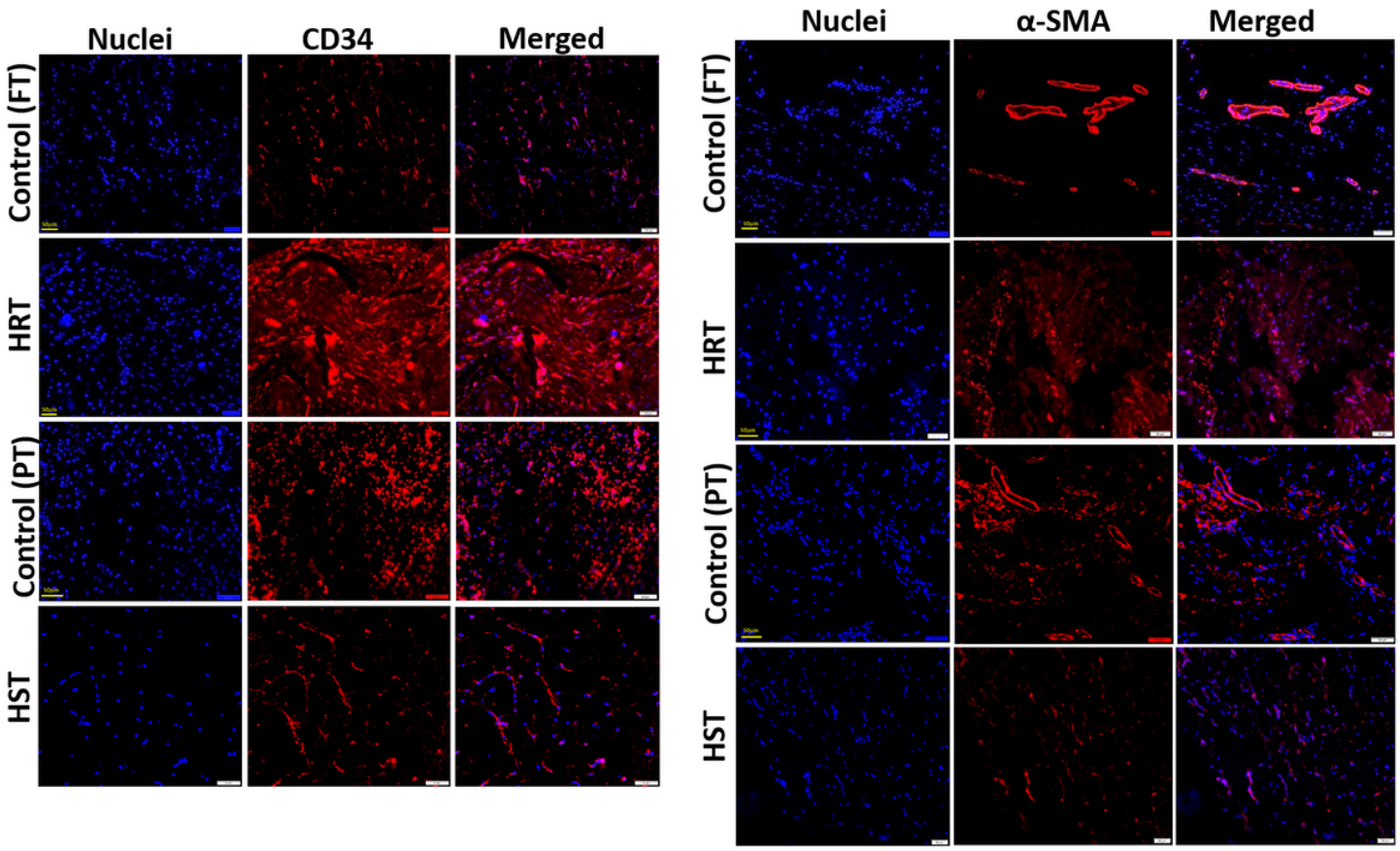

Figure 4

Representative images of the immunofluorescence analysis for the protein expression of CD34 (4A) and α-SMA (4B) of HRT and HST with comparison to controls (FT and PT): Images in the left column show nuclear staining with DAPI; the images in the middle column show expression of the respective biomarker while the images in the right column show overlay of the biomarker staining with DAPI. Images were acquired at 20x magnification (Scale bar - 50μm) using CCD camera attached to the Olympus slide scanner microscope. In CD34 analysis, n=5 for FT, n=4 for PT, n=10 for HST and n=10 for HRT and in α-SMA analysis, n=5 for FT, n=4 for PT, n=10 for HST and n=10 for HRT.

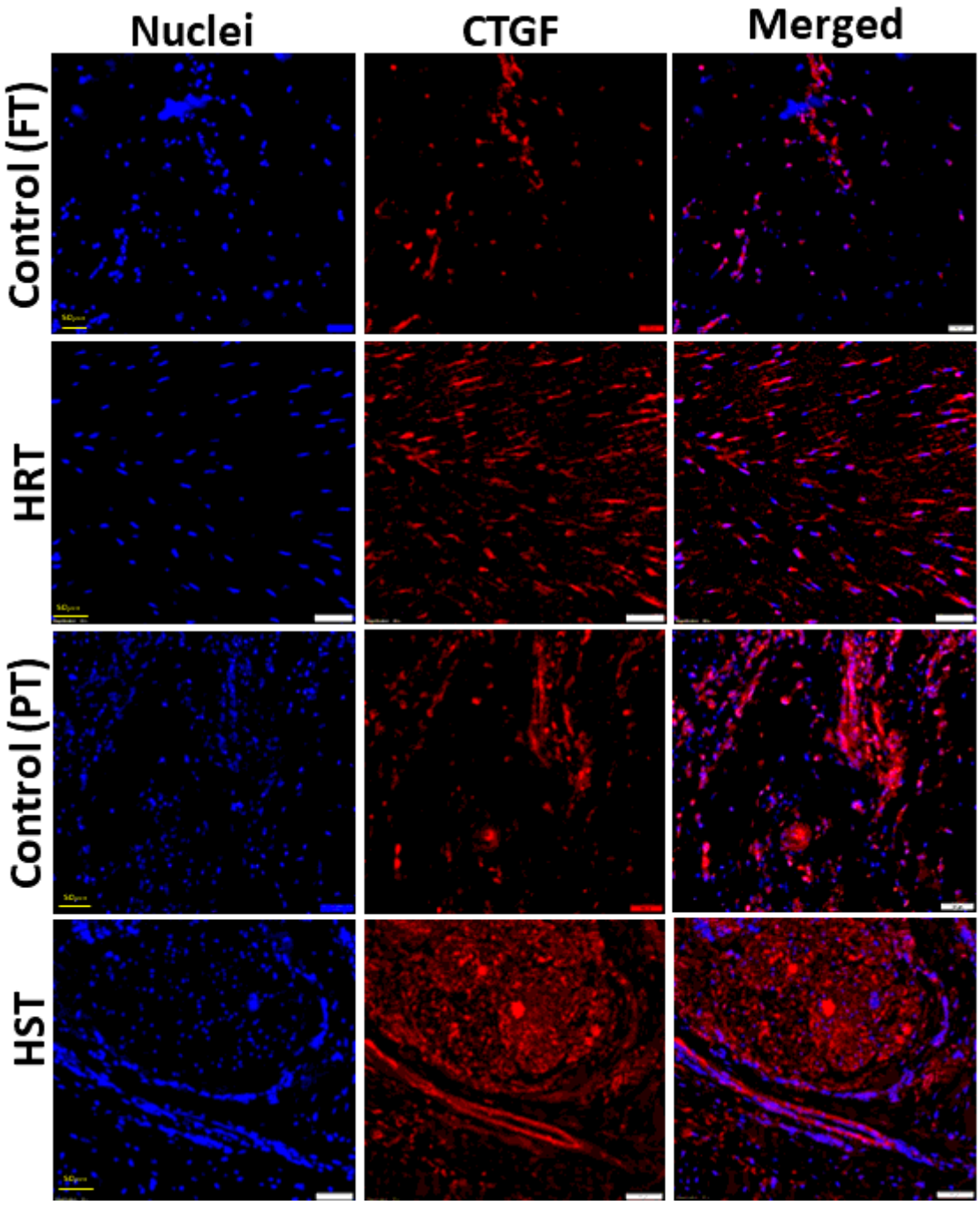

Figure 5

Representative images of the immunofluorescence analysis for the protein expression of CTGF of HRT and HST with comparison to controls (FT and PT): Images in the left column show nuclear staining with DAPI; the images in the middle column show expression of the respective biomarker while the images in the right column show overlay of the biomarker staining with DAPI. Images were acquired at 20x magnification (Scale bar - 50µm) using CCD camera attached to the Olympus slide scanner microscope. In CTGF analysis, n=5 for FT, n=4 for PT, n=10 for HST and n=10 for HRT.

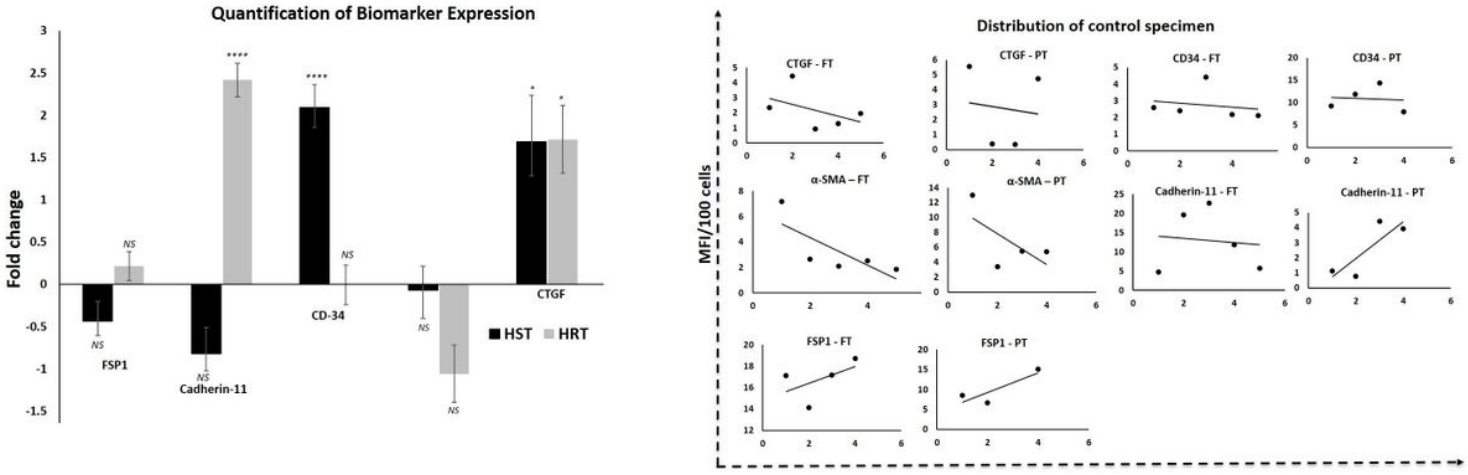

Figure 6

(A) The bar diagram shows quantification of protein expression. The graphs represent mean of fold change of biomarker expression normalized to the control values with standard error. The statistical significance of each control groups vs HRT/HST groups are represented in the figures (NS non-significant, * P<0.05, ** P<0.01, *** P<0.001 and **** P<0.0001). (B) Scatter plot showing the distribution of individual control specimen depicting the variability among the control specimens and the trend.

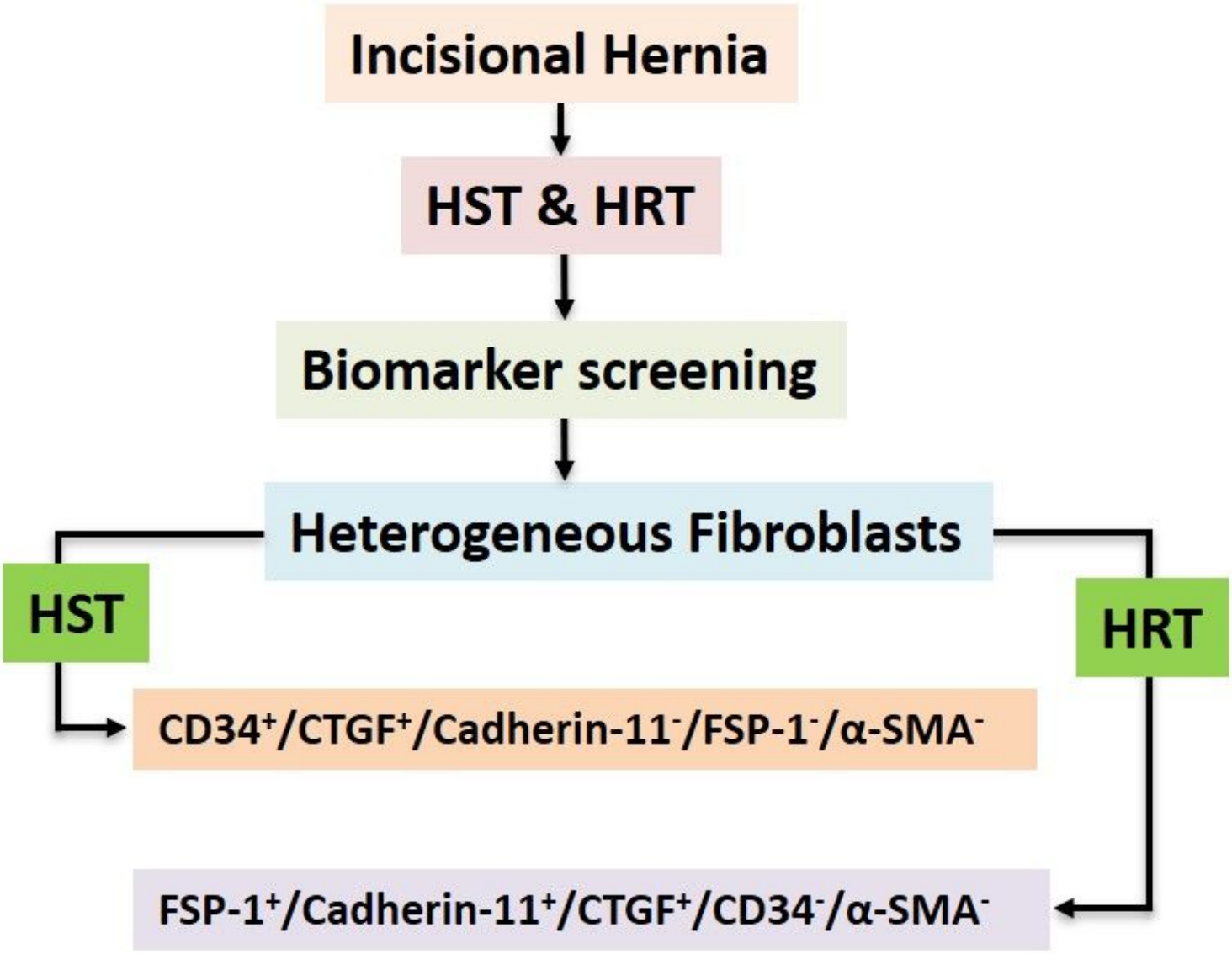

Figure 7

Flow diagram showing the overall findings from the study.

Supplementary Files

This is a list of supplementary files associated with this preprint. Click to download.

- SupportingData.docx